Title TBD

Author List TBD

1 Introduction

Observations of slow-slip and low-frequency earthquakes in nature suggest that fault failure encompasses a spectrum of slip modes [1, 2, 3]. While the explanations for non-traditional earthquakes remain a topic of debate, they have been observed in many subduction zones, including Cascadia [4, 5], Mexico [6], Costa Rica [7], Japan [8], and New Zealand [9]. What causes strain energy to be released across a wide-range of failure behaviors is not understood, and is made more difficult by the limited methods of observation on natural faults. Laboratory stick-slip is often used to model and study repeating earthquake behavior [10, 11]. Frictional stability of a system is predicted to bifurcate at a critical stiffness, k_c [12]. For systems in which $k > k_c$, linearly stable response is expected, while systems with $k < k_c$ are dynamically unstable [13]. Behavior at and near k_c is poorly characterized, but transitional behaviors such as sinusoidal stress variations and slow-slip have been observed [14, 15, 16]. Here we show that critical stiffness is not a fixed parameter, but evolves with shearing, until the material is pushed through a transitory region of conditional stability into traditional fast, stick-slip behavior. We demonstrate stable, slow-slip, and stick-slip behavior in the laboratory by modifying the aggregate shear stiffness of the system.

2 Main

Biaxial double-direct shearing experiments were performed with humidified Min-U-Sil® simulated fault gouge. Force and displacement are recorded on both the normal and shear axes, as well as a measurement of the shearing block position (Fig.1). System compliance can be modified by changing the normal stress (2,4,6,8,12 MPa) or the material of which the central shearing block is made (steel or cast acrylic).

For experiments exhibiting stable sliding behavior, velocity steps were imposed to obtain the rate-and-state frictional parameters of the material and system. The rate-and-state parameters are constants to an empirical fit to transient response of a frictional system to a perturbation [17, 18, 19]. The a parameter provides a measure of the direct effect in response to a velocity step, and b provides the magnitude of friction evolution there-after. The difference of a and b, then yields a quantitative measure of how strongly velocity strengthening or velocity weakening a material is. The critical slip distance, D_c, is often considered to be the slip required to renew the contact population in a granular material. In our experiments, a remains relatively constant with displacement, but b evolves asymptotically upwards with increasing shear displacement. During this transitional period, the critical slip distance evolves downwards (Fig.2).

There are two conditions for unstable behavior to occur: 1) that the material be velocity neutral
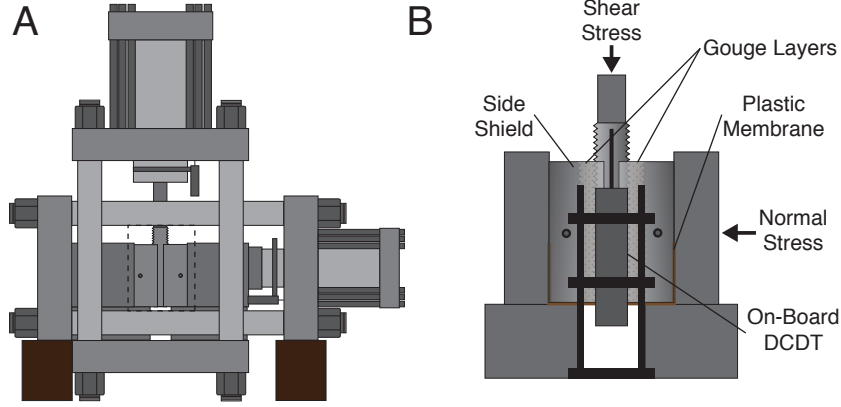
Figure 1: The biaxial deformation apparatus (A) and sample configuration (B). Two large hydraulic pistons are servo-controlled in either force or displacement control modes. Double direct shear samples are supported by steel blocks. Samples use metal side shields and a plastic membrane to reduce gouge extrusion. Local displacement transducers (DCDTs) can be referenced to the center block to avoid apparatus stiffness effects on the measurement.
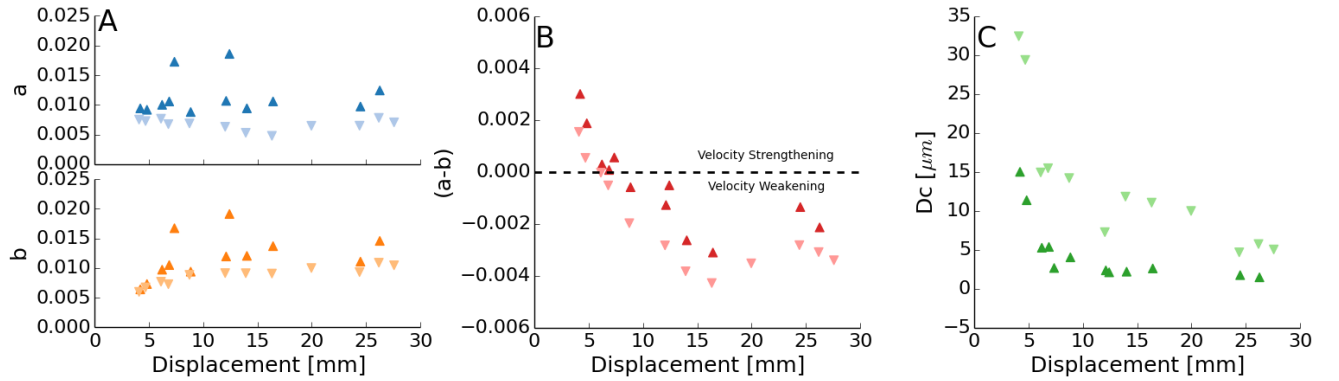

Figure 2: Rate-and-state friction parameters obtained from velocity step inversions. All inversions were accomplished with a fixed stiffness of $k = 5.5 \times 10^{-3} \mu$m. A) rate-and-state parameter a remains relatively constant with displacement and shows a systematic behavior with higher values of a always being observed during velocity up-steps. The b parameter shows a similar behavior, but also increases with displacement, reaching a steady-state value $\sim$10 mm displacement. B) The sample transitions from velocity strengthening to velocity weakening behavior at $\sim$10 mm and remains velocity weakening for the remainder of the experiment. C) Critical slip distance estimates show considerable scatter, but do reduce to a steady-state value of 5-10 um.

to velocity weakening, and 2) that the system stiffness be at or below the critical stiffness [17, 13]. Velocity weakening is a necessary, but insufficient condition for unstable behavior. If a material is velocity strengthening, any acceleration leading to slip is immediately arrested by increased shearing resistance and the energy is frictionally dissipated. The stiffness of the system governs the rate at which energy stored as strain can be released. If the energy release occurs in such a way that the drop in shear resistance with displacement occurs faster than the drop in applied shearing force with displacement, the system can support unstable failure.

In a stiff (all steel) forcing setup, linearly stable frictional behavior was observed. In a more compliant loading system, emergent unstable behavior was observed. Unstable behavior began with frictional oscillations, transitioning to dynamic frictional failure. Oscillations and dynamic failure are characterized by relatively rapid accelerations and decelerations of the system above/below the load point velocity when the material yields under excessive shear force. Experiments with further increased compliance, rapid dynamic failure was observed. These events were audible and classified as fast stick-slip.

The system stiffness was measured, for both stable and unstable experiments, with cycles of unloading and reloading the shear stress at a constant displacement rate of $10\mu m/s$. This provided an estimate of the aggregate system shear stiffness. For experiments that became unstable, a second method of stiffness measurement was employed. Loading stiffnesses of individual slip events were algorithmically determined [16]. We expect both of these methods to provide comparable results and allow determination the system's behavior.

In both determinations of stiffness, we observe increases in measured aggregate system stiffness with accumulated shearing displacement. Unload/reload measurements show these increases are most prevalent in the first 10 mm of shear, asymptotically approaching steady-state. Initial increases in stiffness could be due to layer compaction from grain rearrangement, layer thinning with increased shear strain, grain comminution, localization of shear, or reduction of compliant center block material above the sample due to geometric effects. Layer compaction due to rearrangement and geometric thinning with shear have been well documented [20]. At these low stresses, grain comminution is minimal. Shear localization effects have been shown to play a role in the evolution of layer behavior [21], especially before reaching mechanical steady-state as R and Y shears develop. The reduction in the amount of compliant center block material above the shearing zone with accumulated displacement is minimal compared to these other effects.

Stiffnesses recovered from the loading portion of individual stick-slip events is lower than that from unload/reloads at low displacements. These low values of "working stiffness" do not represent the overall stiffness of the system, but a stiffness influenced by continued slip and creep. As dynamic failure reaches a steady state, we see agreement between the two methods of stiffness measurement (Fig.3).

The transition from velocity strengthening to velocity weakening and corresponding decrease in D_c increase the value of the predicted critical stiffness (eq.1). Combined with increasing system stiffness, a frictional transition is predicted as the critical stiffness intersects the measured system stiffness. We begin to see frictional oscillations and dynamic failure as $k \sim k_c$. The larger the departure from $k = k_c$, the more dramatic the behavior. Very compliant systems exhibit fast dynamic failure. Very stiff systems show no tendency to produced damped oscillations after a velocity step (Fig.4).
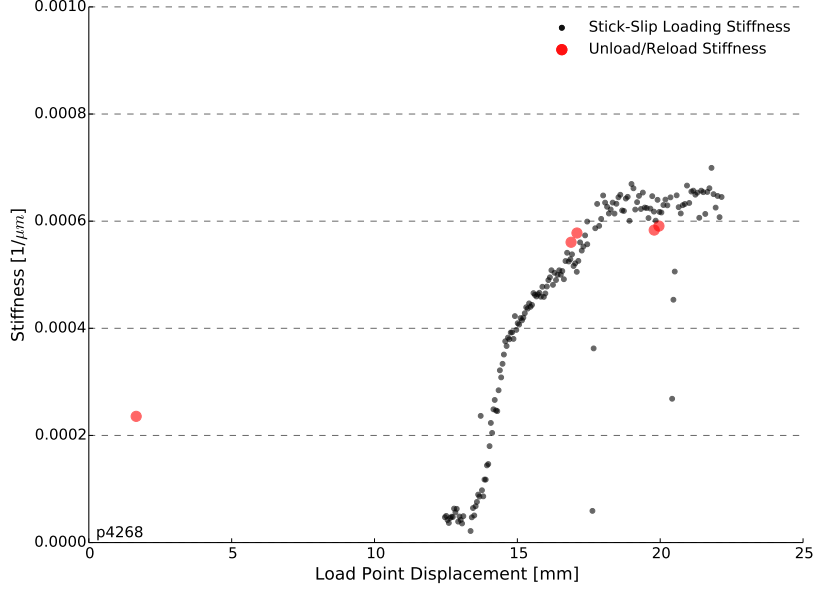
Figure 3: When the sytem is at steady-state, the two methods of stiffness estimation provide comparable results. At low displacements, early stick-slip events appear more compliant than bulk system measurements. This is due to the not fully dynamic failure of the events and creep during the loading phase.

$$k_c = \frac{b - a}{D_c} \tag{1}$$

Our observations of transitional behavior beginning when $k \sim k_c$ suggests that k_c is a valid proxy for the stability of a system, marking a transitory zone between stable sliding and stick-slip that encompasses slow-slip and oscillatory behavior (Fig.5). We also observe that the critical stiffness of a system evolves with shear strain, suggesting that tectonic faults may change behavior as they accumulate slip and become mature fault zones.

In nature, the critical patch size is thought of as the size a crack must grow to before being able to support propagating dynamic rupture. Shallow VLF events in Nankai have been shown to have critical patch sizes of $L_c = 37 - 63$ m, comparable to laboratory tests on natural materials from the area [22]. We likewise calculate patch sizes of 10's of meters for our experiments, but in a simple quartz gouge, not relying on slip dependent clay material properties. The critical patch size (eq.2) grows with increasing k_c and/or increasing normal stress. Extending this to large patch sizes for slow-slip events, and assuming a nominal shear modulus (G), suggests lowered normal stress and/or lowered critical stiffnesses. These arguments are supported by inference of high pore-pressure.

$$r_c = \frac{16}{7\pi} G \frac{D_c}{\sigma_n(b - a)} \tag{2}$$

With slow-slip failure events, we see little to no dynamic overshoot. This is observable by a period of no block motion or deformation after the rapid stress-drop (Fig.4C). In traditional fast stick-slip events, the system shears further than required to complete the force balance. Frictional oscillations and slow-slip show no such overshoot, with continual deformation of the system throughout
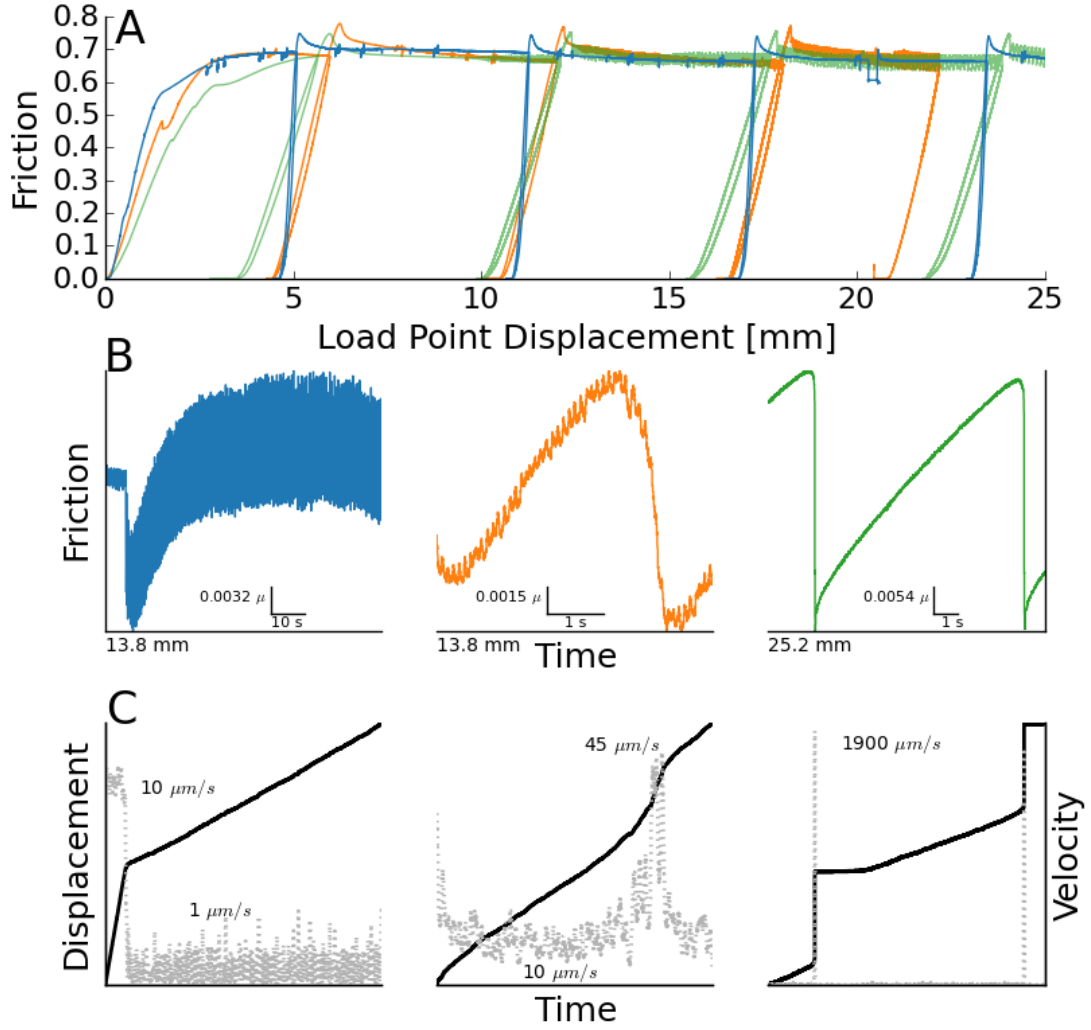
4

Figure 4: A) Run-plots of experiments p4309 (blue), p4311 (orange), and p4316 (green). Different working stiffnesses can be observed as the slope of unload/reload segments. B) All steel blocks produced stable responses to velocity steps (left). Destiffening the system with an acrylic center block produced non-audible slow-slip events (center). Further destiffening with an acrylic center block and increased normal stress produced audible fast stick-slip events(right). C) Center block displacement (black) and velocity (gray) for the corresponding types of failure.
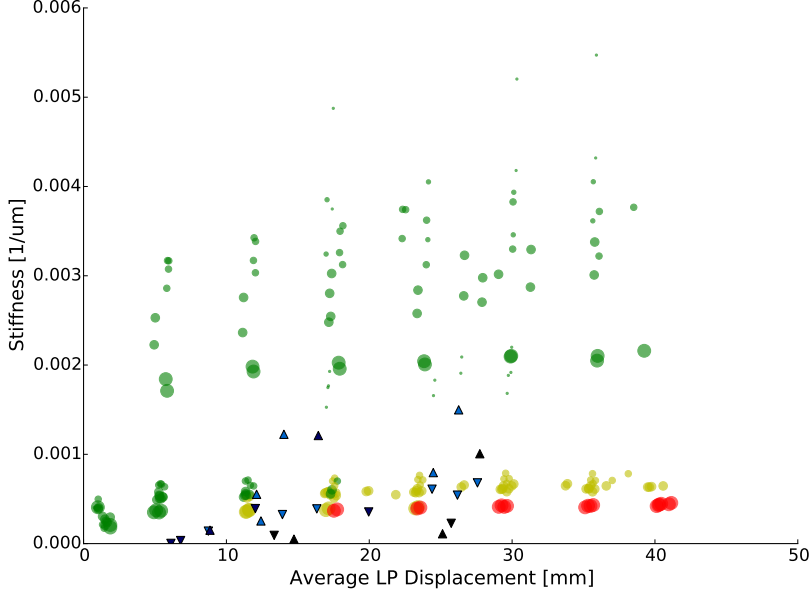
Figure 5: Stiffness estimates from shear stress unload/reload cycles show an increase in the stiffness early in shearing, likely associated with fabric development. Experiments with stiffness comparable to the critical stiffness estimates from velocity steps exhibit slow-slip behavior. Experiments in which the measured stiffness is below the critical stiffness exhibitied more rapid, audible stick-slip.

the simulated seismic cycle. This provides some insight into the low frequency nature of emissions observed from slow-slip and lack of audible report in the laboratory. Lower shear stiffnesses will reduce the seed of rupture propagation, softening step-like acceleration/deceleration pulses that result in high frequency emission. Slowed rupture velocities influence disaster potential, as tsunamogenic earthquake have generally slow rupture velocities [23, 24].

We suggest that where in the spectrum of failure behavior a fault lies can be quantitatively described by the relation of the stiffness of the fault compared to the calculated critical stiffness. While factors such as pore pressure and material frictional response are important, they are already factored into the stiffness comparison. We observe that the critical stiffness of a system evolves as a fabric is developed, suggesting that accumulation of shear can change the behavior of a fault during its lifetime.

3   Methods

All experiments were performed on a servo-controlled biaxial shearing apparatus. Displacements on the normal and shearing axes were measured by Direct Current Displacement Transducers (DCDTs) referenced at the end-platens and ram nose. The displacement of the shearing block was measured with a DCDT referenced at the end-platen and the top of the shearing block. Loads applied to the sample were measured with strain gauge load cells. All transducers are semi-annually calibrated with traceable transfer standards.

Samples were prepared in the double-direct-shear geometry using steel or titanium side blocks and steel or acrylic shearing blocks. All blocks were grooved 0.8 mm deep at 1 mm spacing to reduce

boundary effects [25]. The sample area was 10 x 10 cm and filled with Min-U-Sil to a thickness of 3 mm. Granular layers were left in a sealed container overnight with a solution of anhydrous sodium carbonate to humidify the samples.

After samples were loaded into the load frame, a constant normal stress was applied and maintained by the servo system in a force feedback control mode. Samples were allowed to compact and accomodate grain rearrangement before shearing began. Shearing is conducted at a fixed rate in displacement feedback control mode.

Stiffness of the system was altered by changing the applied normal stress and by changing the material of the shearing block. Increasing normal stress decreases the effective stiffness of the system, as does switching the steel forcing block for a cast acrylic block.

Layers were built of Min-U-Sil$^{®}$ 40 fine ground silica from the U.S. Silica$^{®}$ company Berkeley Springs, West Virginia plant. The median diameter of grain is 10.5 μm. The product is 99.5 % SiO_2, with traces of metal oxides making up the remainder.

System stiffnesses from unload/reload shear stress cycles were calculated by a least-squares linear fit in friction vs. displacement for the interval $\mu = 0.3 - 0.4$. Stiffnesses from the loading portion of slow-slip and stick-slip events were obtained with a derivative based algorithm [16]. Rate-and-state models were fit with both the Dieterich and Ruina laws, with comparable results. Inversions were done with an iterative singular value decomposition technique.

Raw data were recorded in a binary format, and can be read into Python[26]. Processed text output is also available

References

[1] Zhigang Peng and Joan Gomberg. An integrated perspective of the continuum between earthquakes and slow-slip phenomena. *Nature Geosci*, 3(9):599–607, 8 2010.

[2] Satoshi Ide, Gregory C. Beroza, David R. Shelly, and Takahiko Uchide. A scaling law for slow earthquakes. *Nature*, 447(7140):76–9, 5 2007.

[3] Gregory C. Beroza and Satoshi Ide. Slow earthquakes and nonvolcanic tremor. *Annual Review of Earth and Planetary Sciences*, 39(1):271–296, 5 2011.

[4] M. Meghan Miller, Tim Melbourne, Daniel J. Johnson, and William Q. Sumner. Periodic slow earthquakes from the cascadia subduction zone. *Science*, 295(5564):2423–2423, 2002.

[5] Garry Rogers and Herb Dragert. Episodic tremor and slip on the cascadia subduction zone: The chatter of silent slip. *Science*, 300(5627):1942–1943, 2003.

[6] Vladimir Kostoglodov. A large silent earthquake in the guerrero seismic gap, mexico. *Geophysical Research Letters*, 30(15), 2003.

[7] Yan Jiang, Shimon Wdowinski, Timothy H. Dixon, Matthias Hackl, Marino Protti, and Victor Gonzalez. Slow slip events in costa rica detected by continuous gps observations, 2002-2011. *Geochemistry, Geophysics, Geosystems*, 13(4), 4 2012.

[8] Yoshihiro Ito and Kazushige Obara. Very low frequency earthquakes within accretionary prisms are very low stress-drop earthquakes. *Geophysical Research Letters*, 33(9), 2006.

[9] Laura M. Wallace and John Beavan. Diverse slow slip behavior at the hikurangi subduction margin, new zealand. *J. Geophys. Res.*, 115(B12), 2010.

[10] W. F. Brace and J. D. Byerlee. Stick-slip as a mechanism for earthquakes. *Science*, 153(3739):990–992, 1966.

[11] P. A. Johnson, B. Ferdowsi, B. M. Kaproth, M. Scuderi, M. Griffa, J. Carmeliet, R. A. Guyer, P-Y. Le Bas, D. T. Trugman, and C. Marone. Acoustic emission and microslip precursors to stick-slip failure in sheared granular material. *Geophysical Research Letters*, 40(21):5627–5631, 11 2013.

[12] Ji-Cheng Gu, James R Rice, Andy L Ruina, and Simon T Tse. Slip motion and stability of a single degree of freedom elastic system with rate and state dependent friction. *Journal of the Mechanics and Physics of Solids*, 32(3):167–196, 1984.

[13] Christopher H. Scholz. *The mechanics of earthquakes and faulting*. Cambridge University Press, 2002.

[14] Bryan M. Kaproth and C. Marone. Slow earthquakes, preseismic velocity changes, and the origin of slow frictional stick-slip. *Science*, 341(6151):1229–32, 9 2013.

[15] T. Baumberger, F. Heslot, and B. Perrin. Crossover from creep to inertial motion in friction dynamics. *Nature*, 367(6463):544–546, 1994.

[16] J.R. Leeman, M.M. Scuderi, C. Marone, and D.M. Saffer. Stiffness evolution of granular layers and the origin of repetitive, slow, stick-slip frictional sliding. *Granular Matter*, Submitted.

[17] Chris Marone. Laboratory-derived friction laws and their application to seismic faulting. *Annual Review of Earth and Planetary Sciences*, 26(1):643–696, 1998.

[18] James H. Dieterich. Modeling of rock friction: 1. experimental results and constitutive equations. *Journal of Geophysical Research: Solid Earth (1978–2012)*, 84(B5):2161–2168, 1979.

[19] Andy Ruina. Slip instability and state variable friction laws. *Journal of Geophysical Research: Solid Earth (1978–2012)*, 88(B12):10359–10370, 1983.

[20] David R. Scott, Chris J. Marone, and Charles G. Sammis. The apparent friction of granular fault gouge in sheared layers. *Journal of Geophysical Research: Solid Earth*, 99(B4):7231–7246, 1994.

[21] J. M. Logan, C. A. Dengo, N. G. Higgs, and Z. Z. Wang. Fabrics of experimental fault zones: Their development and relationship to mechanical behavior. *International Geophysics*, 51:33–67, 1992.

[22] Matt J. Ikari, Chris Marone, Demian M. Saffer, and Achim J. Kopf. Slip weakening as a mechanism for slow earthquakes. *Nature Geosci*, 6(6):468–472, 5 2013.

[23] Hiroo Kanamori and Masayuki Kikuchi. The 1992 nicaragua earthquake: a slow tsunami earthquake associated with subducted sediments. *Nature*, 361(6414):714–716, 1993.

[24] Susan L. Bilek and Thorne Lay. Rigidity variations with depth along interplate megathrust faults in subduction zones. *Nature*, 400(6743):443–446, 1999.

[25] Jennifer L. Anthony and Chris Marone. Influence of particle characteristics on granular friction. *Journal of Geophysical Research: Solid Earth*, 110(B8), 2005.

[26] J.R. Leeman. biaxread 1.0.1 - python data reader. https://github.com/jrleeman/biaxread doi:10.5281/zenodo.9963, 2014.

4 Acknowledgements

5 Author Contributions

All authors contributed to data interpretation, analysis schema, and writing. J. Leeman conducted experiments and data analysis.

6 Competing Financial Interests

The authors declare no competing financial interests. Supplementary information accompanies this paper on www.nature.com/naturegeoscience. All data is avaliable for download, as well as Python scripts/notebooks to replicate data analysis on GitHub (www.github.com/jrleeman). Reprints and permissions information is available online at http://npg.nature.com/reprintsandpermissions. Correspondence and requests for materials should be addressed to J. Leeman.